Numerical solution of stochastic differential equations with Poisson and Lévy white noise

M. Grigoriu
Cornell University, Ithaca, New York 14853-3501, USA
(Received 3 April 2009; published 21 August 2009)

A fixed time step method is developed for integrating stochastic differential equations (SDE's) with Poisson white noise (PWN) and Lévy white noise (LWN). The method for integrating SDE's with PWN has the same structure as that proposed by Kim *et al.* [Phys. Rev. E **76**, 011109 (2007)], but is established by using different arguments. The integration of SDE's with LWN is based on a representation of Lévy processes by sums of scaled Brownian motions and compound Poisson processes. It is shown that the numerical solutions of SDE's with PWN and LWN converge weakly to the exact solutions of these equations, so that they can be used to estimate not only marginal properties but also distributions of functionals of the exact solutions. Numerical examples are used to demonstrate the applications and the accuracy of the proposed integration algorithms.

DOI: 10.1103/PhysRevE.80.026704 PACS number(s): 02.70.−c, 02.50.−r

I. INTRODUCTION

Stochastic differential equations (SDE's) are used extensively in applied sciences and engineering to describe the behavior of physical, biological, engineering, and other systems. For example, noise-induced transitions in physics, chemistry, and biology can be captured by changes in the probability law of the solutions of SDE's with Gaussian white noise (GWN) ([1], Chapter 7, [2]), stability of dynamic systems in Gaussian random environment can be inferred from Lyapunov exponents calculated for solutions of SDE's with multiplicative GWN ([2], Sec. 8.7), and predictions of a system state can be improved by accounting for observations of its state via filtering theory for SDE's with GWN [3,4].

The solutions of SDE's with GWN are continuous stochastic processes so that they cannot be used to describe phenomena exhibiting jumps of random magnitude occurring at random times. For example, earth temperature X is strongly correlated with calcium concentration whose records over 80 000 years exhibit large jumps corresponding to the interstadial and the full glacial states [5]. It has been proposed to model earth temperature X by a stochastic process satisfying a stochastic differential equation driven by GWN and Lévy white noise (LWN). The drift coefficient of this equation corresponds to a potential with two wells associated with the interstadial and the full glacial states. The jumps of X between potential wells is facilitated by the Lévy white noise that has been scaled such that the typical residence of X in a potential well is between 1000 and 2000 years [5]. Similar models have been used to characterize sea surface temperature $T(t)$ in the Southern Pacific. For example, $T(t)$ has been described by the first coordinate of a two-dimensional diffusion process with nonlinear drift driven by GWN whose second coordinate is the physically active surface layer of the ocean [6]. Stochastic differential equations with Poisson white noise (PWN) have been used in a broad range of applications to describe the motion of particles in spatially periodic potential [7], find the response of nonlinear dynamic systems to PWN [8,9], and assess the stability of the solution of stochastic differential equations with multiplicative PWN via Lyapunov exponents [10].

The development of algorithms for solving stochastic differential equations with GWN is rather straightforward. Even recurrence formulas derived from the Euler forward scheme are satisfactory provided the integration time step is sufficiently small. Superior integration schemes can be found in [11]. Most Monte Carlo algorithms for solving stochastic differential equations with GWN have a constant time step. In contrast, fixed time step algorithms cannot be used directly to integrate SDE's with PWN since the pulses of PWN processes arrive at random times. Variable time step algorithms are needed to integrate SDE's with PWN. This constraint prevents the development of general numerical methods for integrating SDE's subject to, for example, Gaussian and Poisson white noise.

There are significant theoretical studies on the convergence of Euler integration schemes for stochastic differential equations driven by PWN and/or LWN. For example, the strong convergence and stability of these schemes has been established in [12] for SDE's with PWN with drift coefficients that may not satisfy global Lipschitz conditions. Theorems on the accuracy of Euler integration schemes for SDE's driven by LWN can be found in [13,14]. However, the numerical implementation of the available theoretical results is rather limited. A notable exception is the numerical method with fixed time step proposed in [7] to integrate SDE's with PWN that resembles algorithms used to integrate SDE's driven by GWN. The accuracy of the method proposed in this reference has been demonstrated by numerical examples.

We present an alternative of the fixed time step method in [7] that can be used to integrate SDE's with both PWN and LWN. Our specific objectives are to (1) develop a method for integrating SDE's with PWN that, as the method in [7], has a fixed time step but is derived using arguments different from those in [7]; (2) extend the method for integrating SDE's with PWN to the class of SDE's with LWN by representing a Lévy process as a sum of a scaled Brownian motion and a compound Poisson process; (3) prove the convergence of the proposed numerical solution to the exact solution of stochastic differential equations driven by PWN and LWN; and (4) demonstrate the application and the accuracy of the proposed method by numerical examples.

II. PROBLEM DEFINITION

Let X be a real-valued stochastic process defined by the Itô stochastic differential equation

$$dX(t) = \mu[X(t)]dt + \sigma[X(t)]dY(t), \quad t \geq 0, \tag{1}$$

where the driving noise Y can be a standard Brownian motion B, a compound Poisson process C, or a symmetric α-stable Lévy motion process L_α, $\alpha \in (0,2]$. It is common to refer to the formal derivatives of B, C, and L_α as Gaussian (GWN), Poisson (PWN), and Lévy (LWN) white noise processes. It is assumed that the drift and diffusion coefficients μ and σ are such that the solution X of Eq. (1) exists and is unique.

The processes B, C, and L_α have similar and notably different properties. For example, B, C, and L_α have stationary independent increments but these increments follow different distributions. The increments $B(t)-B(s)$, $t>s$, of B are Gaussian variables with mean 0 and variance $t-s$. The increments $L_\alpha(t)-L_\alpha(s)$, $t>s$, of L_α are symmetric α-stable random variables with characteristic functions $\varphi_{L_\alpha(t)-L_\alpha(s)}(u)=\exp[-(t-s)|u|^\alpha]$, $u \in \mathbb{R}$, so that $L_2(t)-L_2(s)$ is a Gaussian variable with mean 0 and variance $2(t-s)$. The compound Poisson process C is defined by

$$C(t) = \sum_{k=1}^{N(t)} Y_k, \quad t \geq 0, \tag{2}$$

where N is a homogeneous Poisson process with intensity $\lambda > 0$ and $\{Y_k\}$ are independent identically distributed (iid) random variables. Accordingly, the characteristic function of an increment $C(t)-C(s)$ of C is $\varphi_{C(t)-C(s)}(u)=\exp[-\lambda(t-s)(1-\varphi_{Y_1}(u))]$, $u \in \mathbb{R}$, where φ_{Y_1} denotes the characteristic function of Y_1. We also note that B has continuous samples and so does the solution X in Eq. (1) with B in place of Y. On the other hand, the samples of C and L_α exhibit jumps that are mapped into jumps of the solutions of Eq. (1) driven by PWN and LWN.

The fixed time step integration method proposed in this study is based on the representation of the driving process Y in Eq. (1) by sequences of random walks

$$Y_n(t) = \sum_{k=1}^{[t/\Delta t_n]} Z_{n,k}, \quad t \geq 0, \quad n = 1,2, \ldots, \tag{3}$$

where $\Delta t_n = \tau/n$, $[0,\tau]$ denotes an integration interval, $[\xi]$ denotes the largest integer smaller than ξ, and $\{Z_{n,k}\}$ are independent identically distributed random variables.

Let X_n be the solution of Eq. (1) with Y_n in place of Y, that is, X_n satisfies the stochastic differential equation

$$dX_n(t) = \mu[X_n(t)]dt + \sigma[X_n(t)]dY_n(t), \quad t \geq 0. \tag{4}$$

We construct random walk sequences similar to Y_n in Eq. (3) for B, C, and L_α, and show that the resulting sequences converge weakly to B, C, and L_α as $\Delta t_n \to 0$. The weak convergence of Y_n to Y, denoted by $Y_n \Rightarrow Y$, is used to prove the weak convergence $X_n \Rightarrow X$ of the sequence of approximate solutions X_n of Eq. (1) to the exact solution X of this equation as $\Delta t_n \to 0$. The property $X_n \Rightarrow X$ allows us to approximate not only statistics of X at an arbitrary time t, that is, statistics of random variable $X(t)$, from samples of $X_n(t)$ but also distributions of functionals of X, for example, $\max_{0\leq t\leq \tau}|X(t)|$, from samples of X_n provided the time step Δt_n is sufficiently small.

The integral version of Eq. (4) in a time interval $(t_{k-1}, t_k]$ is

$$X_n(t_k) = X_n(t_{k-1}) + \int_{t_{k-1}}^{t_k} \mu[X_n(s)]ds + \sigma[X_n(t_{k-1})]Z_{n,k-1},$$
$$k = 1,2, \ldots, \tag{5}$$

which yields the recurrence formula

$$X_{n,k} = X_{n,k-1} + \mu(X_{n,k-1})\Delta t_n + \sigma(X_{n,k-1})Z_{n,k-1}, \quad k = 1,2, \ldots, \tag{6}$$

where $X_{n,k}$ is an approximation of $X_n(t_k)$, $t_k = k\Delta t_n$, $k=1,\ldots,n$, and $t_0=0$.

III. RANDOM WALK MODELS AND RECURRENCE FORMULAS

We define sequences of random walk models for B, C, and L_α corresponding to time steps $\Delta t_n = \tau/n$ similar to the model Y_n of Y in Eq. (3), where $[0,\tau]$ denotes an integration time interval. The random walk models of B, C, and L_α are subsequently used to develop recurrence formulas of the type in Eq. (6) for integrating SDE's with GWN, PWN, and LWN.

A. Random walk models

Let

$$B_n(t) = (\Delta t_n)^{1/2} \sum_{k=1}^{[t/\Delta t_n]} G_k, \quad t \geq 0, \tag{7}$$

be a sequence of random walks with time step Δt_n approximating the Brownian motion B, where $\{G_k\}$ are independent standard Gaussian variables. We note that $B_n(t)$ is a Gaussian random variable with mean 0 and variance $\Delta t_n[t/\Delta t_n] = t[t/\Delta t_n]/(t/\Delta t_n)$ converging to t as $n \to \infty$, so that the random variables $B_n(t)$ and $B(t)$ have the same distribution as $n \to \infty$ or, equivalently, $\Delta t_n \to 0$.

Consider the compound Poisson process C in Eq. (2), and let

$$C_n(t) = \sum_{k=1}^{[t/\Delta t_n]} V_{n,k}, \quad t \geq 0, \tag{8}$$

be a sequence of random walks approximating C, where $C_n(0)=0$, $\Sigma_{k=1}^{0} V_{n,k}=0$ by convention, and

$$V_{n,k} = \begin{cases} \text{an independent copy of } Y_1, & \text{probability } p_n = 1 - e^{-\lambda \Delta t_n} \\ 0, & \text{probability } 1 - p_n. \end{cases} \tag{9}$$

are iid random variables. The mean and variance of $C_n(t)$ are equal to $[t/\Delta t_n]E[V_{n,1}]=[t/\Delta t_n]p_n E[Y_1]$ and $[t/\Delta t_n]\mathrm{Var}[V_{n,1}]=[t/\Delta t_n]p_n \mathrm{Var}[V_{n,1}]$ and converge to $\lambda t E[Y_1]$ and $\lambda t E[Y_1^2]$ as $\Delta t_n \to 0$, so that the random variables $C_n(t)$ and $C(t)$ have the same mean and variance as $\Delta t_n \to 0$. We note that the representation in Eqs. (8) and (9) is valid asymptotically as $\Delta t_n \to 0$ and is numerically accurate for $p_n \ll 1$, or equivalently, $\lambda \Delta t_n \ll 1$, as illustrate by a numerical example presented in a subsequent section.

We construct two distinct random walk sequences approximating the α-stable process L_α. The first sequence is similar to that in Eq. (7), and is defined by

$$L_{\alpha,n}(t) = (\Delta t_n)^{1/\alpha} \sum_{k=1}^{[t/\Delta t_n]} S_k, \quad t \geq 0, \tag{10}$$

where $\{S_k\}$ are iid symmetric α-stable random variables with characteristic function $\varphi_{S_1}(u)=\exp(-|u|^\alpha)$, $u \in \mathbb{R}$. If $\alpha=2$, the random variables $\{S_k\}$ are Gaussian with mean 0 and variance 2.

The second random walk sequence approximating L_α is based on the approximate representation

$$L_\alpha(t) \simeq L^{(\alpha,a)}(t) = \gamma(\alpha,a)B(t) + C^{(\alpha,a)}(t), \tag{11}$$

of this process developed in [15], which states that any α-stable process can be viewed as a sum of two independent processes, a scaled Brownian motion and a compound Poisson process $C^{(\alpha,a)}$, where $a>0$ is arbitrary. The scale of the Brownian motion is given by

$$\gamma(\alpha,a)^2 = \int_{-a}^{a} y^2 \lambda_L(dy) = \frac{\alpha}{2-\alpha} c_\alpha a^{2-\alpha}. \tag{12}$$

The Poisson component of L_α is the compound Poisson process

$$C^{(\alpha,a)}(t) = \sum_{k=1}^{N^{(\alpha,a)}(t)} Y_k^{(\alpha,a)}, \tag{13}$$

where $N^{(\alpha,a)}$ is a Poisson counting process with intensity $\lambda^{(\alpha,a)}=c_\alpha/a^\alpha$,

$$c_\alpha = \begin{cases} \dfrac{1-\alpha}{\Gamma(2-\alpha)\cos(\pi\alpha/2)}, & \text{if } \alpha \neq 1 \\ 2/\pi & \text{if } \alpha = 1, \end{cases} \tag{14}$$

and $\{Y_k^{(\alpha,a)}\}$ are independent identically distributed random variables ([16], Property 1.2.15). The random variables $\{Y_k^{(\alpha,a)}\}$ correspond to the jumps of $L_\alpha(t)$ with magnitude exceeding a, referred to as the large jumps of L_α. The distribution, the density, and the characteristic functions of $Y_1^{(\alpha,a)}$ are [17]

$$F_a(y) = \frac{\alpha a^\alpha}{2}\left[\frac{1}{\alpha|y|^\alpha}1(y<-a) + \frac{1}{\alpha a^\alpha}1(y \geq -a) + \frac{1-(a/y)^\alpha}{\alpha a^\alpha}1(y \geq a)\right], \quad y \in \mathbb{R}, \tag{15}$$

$$f_a(y) = \frac{\alpha a^\alpha}{2}[|y|^{-(\alpha+1)}1(y<-a) + y^{-(\alpha+1)}1(y \geq a)], \quad y \in \mathbb{R}, \tag{16}$$

and

$$\varphi_a(u) = \alpha a^\alpha \int_a^\infty \cos(uy) y^{-(\alpha+1)} dy, \quad u \in \mathbb{R}, \tag{17}$$

respectively. The accuracy of the approximation $L_\alpha(t) \simeq L^{(\alpha,a)}(t)$ in Eq. (11) is remarkable [17], so that we will not distinguish between these two processes. Accordingly, the second random walk model of L_α is constructed for $L^{(\alpha,a)}$ in Eq. (11) rather than L_α and is

$$L_n^{(\alpha,a)}(t) = \gamma(\alpha,a)B_n(t) + C_n^{(\alpha,a)}(t), \quad t \geq 0, \tag{18}$$

where B_n is given by Eq. (7), the scale $\gamma(\alpha,a)$ is in Eq. (12),

$$C_n^{(\alpha,a)}(t) = \sum_{k=1}^{[t/\Delta t_n]} V_{n,k}^{(\alpha,a)}, \quad t \geq 0, \tag{19}$$

and $\{V_{n,k}^{(\alpha,a)}\}$ are independent random variables given by Eq. (9) with $Y_1^{(\alpha,a)}$ and $\lambda^{(\alpha,a)}$ in place of Y_1 and λ, respectively. We also note that the scale $\gamma(\alpha,a)$ of the Brownian component and the intensity $\lambda^{(\alpha,a)}$ of the jumps of the compound Poisson component of the Lévy white noise increase and decrease with a, respectively. Accordingly, we can select a value of a such that $\lambda^{(\alpha,a)}\Delta t_n$ be sufficiently small for the representation of $C_n^{(\alpha,a)}$ in Eq. (19) to hold.

B. Recurrence formulas

The approximate solution X_n of X in Eq. (1) satisfies the stochastic integral equation given by Eq. (5) with

$$Z_{n,k-1} = \begin{cases} (\Delta t_n)^{1/2} G_{k-1}, & \text{for GWN} \\ V_{n,k-1}, & \text{for PWN} \\ (\Delta t_n)^{1/\alpha} S_{k-1}, & \text{for LWN(first representation)} \\ (\Delta t_n)^{1/2} \gamma(\alpha,a) G_{k-1} + V_{n,k-1}^{(\alpha,a)}, & \text{for LWN(second representation),} \end{cases} \tag{20}$$

corresponding to the random walk models in Eqs. (7)–(14). One of our objectives is to show that X_n converges weakly to the solution X of Eq. (1) as the time step Δt_n of the random walks approximating the driving processes B, C, or L_α decreases to 0. As previously stated, this convergence guarantees that statistics of X and functionals of this process can be estimated from samples of X_n for a sufficiently small time step Δt_n.

The recurrence formula in Eq. (6) with $Z_{n,k-1}$ in Eq. (20) can be used to generate samples of $X_{n,k}$ driven by GWN, PWN, or LWN. For example, this formula is

$$X_{n,k} = X_{n,k-1} + \mu(X_{n,k-1})\Delta t_n + \sigma(X_{n,k-1}) \times [(\Delta t_n)^{1/2}\gamma(\alpha,a)G_{k-1} + V_{n,k-1}^{(\alpha,a)}], \quad k = 1,2, \ldots, \tag{21}$$

for the case of Lévy white noise described by the random walk model in Eq. (18). We note that (i) the proposed algorithms for integrating Eq. (1) have the same structure irrespective of the noise type, (ii) the method for integrating Eq. (1) with LWN described by its model in Eq. (18) results from the integration schemes of this equation driven by GWN and PWN processes, and (iii) both random walk models of L_α can be used to integrate Eq. (1) with LWN. The random walk model of L_α in Eq. (10) has been used extensively in applications with good results ([18–20] Sec. 4.8).

We prefer the representation of L_α in Eq. (18) since the integration time step Δt_n can be selected simply from the condition $\lambda^{(\alpha,a)}\Delta t_n \ll 1$ and classical requirements for SDE's driven by GWN. In contrast, the selection of Δt_n for the random walk model in Eq. (10) is rather difficult since the intensity of the small Lévy processes is unbounded. Moreover, the model in Eq. (10) requires to generate samples of heavy tail distributions at each time step rather than at every $1/(\lambda^{(\alpha,a)}\Delta t_n)$ time step on average, and the generation of samples from these distributions can encounter numerical difficulties. For example, samples of a standard α-stable random variable with $\alpha=1$, that is, a Cauchy variable, can be generated from $\tan(U)$, where U is uniformly distributed in the range $(-\pi/2,\pi/2)$. To avoid numerical difficulties, we need to generate samples from $\tan(\tilde{U})$ rather than $\tan(U)$, where $\tilde{U}$ is uniformly distributed in $[-\pi/2+\varepsilon, \pi/2-\varepsilon]$ and $\varepsilon > 0$ is small. The selection of an adequate value for $\varepsilon > 0$ is not trivial, and may require iterations.

IV. CONVERGENCE OF APPROXIMATE SOLUTIONS

We show that the random walk sequences B_n, C_n, and $L_n^{(\alpha,a)}$ converge weakly to B, C, and $L^{(\alpha,a)}$ as $n\to\infty$ or, equivalently, $\Delta t_n \to 0$, and denote these properties by $B_n \Rightarrow B$, $C_n \Rightarrow C$, and $L_n^{(\alpha,a)} \Rightarrow L^{(\alpha,a)}$. The convergence of these sequences of processes is used to show that the solutions X_n of Eq. (4) converges weakly to the solution X of Eq. (1). As previously stated, the weak convergence $X_n \Rightarrow X$ allows us to approximate not only marginal statistics of X, for example, the marginal distribution this process as in [7], but also distributions of functionals of X, for example, the distribution of $\max_{0\le t\le\tau} X(t)$ or $\int_0^\tau h[X(t)]dt$ for measurable functions $h:\mathbb{R}\to\mathbb{R}$, from samples of X_n for a sufficiently large n. The mean square convergence of the sequence of random variables $X_n(\tau)$ to $X(\tau)$ as $n\to\infty$ does not guarantee that statistics of functionals of X can be approximated by statistics of corresponding functionals of X_n.

Consider first the convergence of the driving noise processes. Since B_n is a Gaussian sequence and has stationary independent, it has the same finite dimensional distributions as B asymptotically as $n\to\infty$. The weak convergence $B_n \Rightarrow B$ results from [21] (Corollary 1 to Theorem 5.1).

We only summarize the main steps of a proof of the weak convergence of C_n to C, and provide some technicalities of the proof in the Appendix. The characteristic function of $C_n(t)$ is

$$\varphi_n(u;t) = E[e^{iuC_n(t)}] = \varphi_{V_{n,1}}(u)^m = [(1-e^{-\lambda\Delta t_n})\varphi_{Y_1}(u) + e^{-\lambda\Delta t_n}]^m \tag{22}$$

by properties of $\{V_{n,k}\}$, where $m=[t/\Delta t_n]$, $\varphi_{V_{n,1}}$ denotes the characteristic function of $V_{n,1}$, and φ_{Y_1} is the characteristic function of Y_1. For $\lambda\Delta t_n \ll 1$ with the notation $\beta=\lambda[\varphi_{Y_1}(u)-1]$, we have $\varphi_n(u;t)=[1+\beta\Delta t_n+O(\Delta t_n)^2]^m$ so that

$$\lim_{n\to\infty} \varphi_n(u;t) = \exp\{-\lambda t[1-\varphi_{Y_1}(u)]\} = E[e^{iuC(t)}] = \varphi(u;t). \tag{23}$$

This result show that C_n and C have the same marginal distributions asymptotically as $n\to\infty$, and implies the convergence of the finite dimensional distributions of C_n to those of C since these processes have stationary independent increments ([2], Sec. 3.6.4). The weak convergence $C_n \Rightarrow C$ follows from these properties of C_n and technical arguments presented in the Appendix.

The weak convergence $L_n^{(\alpha,a)} \Rightarrow L^{(\alpha,a)}$ follows from the above properties of B_n and C_n. We have seen that the sequence of random walk processes C_n defined by Eq. (8) converges weakly to C in Eq. (2). This implies the weak convergence $C_n^{(\alpha,a)} \Rightarrow C^{(\alpha,a)}$ for any $a>0$. The weak convergence $\gamma(\alpha,a)B_n \Rightarrow \gamma(\alpha,a)B$ is implied by $B_n \Rightarrow B$ discussed previously.

Consider now the convergence $X_n \Rightarrow X$. The processes X and X_n are defined by the stochastic integral equations

$$X(t) = \int_0^t \rho[X(s)]dY^*(s)$$

$$X_n(t) = \int_0^t \rho[X_n(s)]dY_n^*(s) \tag{24}$$

for zero initial state, where $\rho[X(t)]$ and $\rho[X_n(t)]$ are (2,2) diagonal matrices with nonzero entries $\mu[X(t)]$; $\sigma[X(t)]$ and $\mu[X_n(t)]$; $\sigma[X_n(t)]$, and $Y^*(t)$ and $Y_n^*(t)$ are two-dimensional column vectors with the first coordinates the identity function $i(t)=t$ and the second coordinates $B(t)$ and $B_n(t)$, $C(t)$ and $C_n(t)$, $L_\alpha(t)$ and $L_{\alpha,n}(t)$, or $L^{(\alpha,a)}(t)$ and $L_n^{(\alpha,a)}(t)$, respectively, depending on the noise type. The assumption of zero initial state is not restrictive since $X(0)=X_n(0)$.

The essentials steps of the proof that X_n converges weakly to X are in the Appendix. We only mention here that the sequence of processes Y_n^* converges weakly to Y^* since these processes have the same first coordinate and the second coordinate of Y_n^* converges weakly to that Y^*. The convergence $Y_n^* \Rightarrow Y^*$ and technical arguments in [22] are used in the Appendix to prove the convergence $X_n \Rightarrow X$.

V. NUMERICAL EXAMPLES

We apply the proposed numerical methods to integrate stochastic differential equations driven by PWN and LWN. The first example is a SDE with PWN taken from [7]. The second example is a SDE driven by LWN. Analytical solutions are available for the stationary distribution of X in both examples, and these solutions are used to assess the accuracy of the integration algorithms proposed in this study.

A. Poisson white noise

Consider Eq. (1) with $\mu(x)=-v'(x)$ for $x\in[-L/2,L/2]$, $\sigma(x)=1$, and $Y=C$, where $v(x)=|x|$ implying $\mu(x)=-\text{sgn}(x)$. Since the diffusion coefficient does not depend on X, we say that the driving noise is additive. As in [7], we use periodic boundary conditions that are defined as follows for the discrete approximation $\{X_{n,k}\}$ of the state X of Eq. (1). Let $X_{n,k}(\omega)$ be a sample of $X_{n,k}$ and suppose that $X_{n,k-1}(\omega)\in[-L/2,L/2]$. If $X_{n,k}(\omega)\notin[-L/2,L/2]$, then $X_{n,k}(\omega)$ is mapped into $X_{n,k}(\omega)=-\text{sgn}(L/2-\xi)(L/2-\xi)$, where $\xi=\xi_0-[\xi_0/L]L$ and $\xi_0=|X_{n,k}(\omega)|-L/2$. For example, if $X_{n,k}(\omega)=5L/8$, then $\xi_0=L/8$ and $\xi=\xi_0=L/8$ so that we set $X_{n,k}(\omega)=-\text{sgn}(L/2-L/8)(L/2-L/8)=-3L/8$. These periodic boundary conditions assure that the samples of $X_{n,k}$ are in the range $[-L/2,L/2]$ at all times.

Numerical results have been obtained for a compensated compound Poisson process with exponential jumps, that is, $C(t)$ in Eq. (1) is replaced by $C(t)-E[C(t)]=C(t)-\lambda tE[Y_1]$. As in [7], the jumps of $C(t)$ are exponential random variable with decay parameter $\eta>0$ and mean $E[Y_1]=1/\eta$. The corresponding version of the recurrence formula in Eq. (6) is

$$X_{n,k} = X_{n,k-1} - \text{sgn}(X_{n,k-1})\Delta t_n + V_{n,k-1} - \lambda E[Y_1]\Delta t_n. \tag{25}$$

The noise strength is denoted by $D=\lambda\ \text{Var}[Y_1]=\lambda/\eta^2$ and is set equal to 1 in all numerical examples. As in [7], numerical results have been obtained for $\lambda=0.5$, 1, 2, and 100 yielding $\eta=1/\sqrt{\lambda}=1/\sqrt{0.5}=1.4142$, 1.0, 0.7071, and 0.1. Hence, the driving noise has large and rare jumps for small values of λ and small and frequent jumps for large values of λ.

Figure 1 shows histograms of the stationary state $X_{n,k}$ based on 10^5 independent samples of this process generated in a time interval $(0,\tau]$, $\tau=10$, with a time step $\Delta t_n=0.01$ corresponding to a partition of $(0,\tau]$ in $n=1000$ equal intervals for $\lambda=0.5$, 1, and 2. The time step had to be decreased to $\Delta t_n=0.0001$ for $\lambda=100$ to obtain accurate results, in agreement with previous comments related to the representation in Eqs. (8) and (9). The plots in Fig. 1 match the histograms and the analytical results in [7]. We note that the recurrence formula used in this reference to integrate Eq. (1) results from the integral form,

$$X(t_k) = X(t_{k-1}) + \int_{t_{k-1}}^{t_k} \mu[X(s)]ds + \int_{t_{k-1}}^{t_k} \sigma[X(s)]dC(s), \tag{26}$$

of this equation for an interval $(t_{k-1},t_k]$ and the approximations $\int_{t_{k-1}}^{t_k}\mu[X(s)]ds \simeq \mu[X(t_{k-1})]\Delta t_n$ and $\int_{t_{k-1}}^{t_k}\sigma[X(s)]dC(s) \simeq \sigma[X(t_{k-1})]\Delta C_{k-1}=\sigma[X(t_{k-1})][C(t_k)-C(t_{k-1})]$, and has the expression

$$\tilde{X}_k = \tilde{X}_{k-1} + \mu(\tilde{X}_{k-1})\Delta t + \sigma(\tilde{X}_{k-1})\Delta C_{k-1}, \tag{27}$$

where $\tilde{X}_k$ is an approximation of $X(t_k)$, $\Delta t=t_k-t_{k-1}$, and $\Delta C_{k-1}=\int_{t_{k-1}}^{t_k}dC(s)$. The equality in Eq. (27) resembles the classical recurrence formula for generating samples of the solutions of SDE's with GWN [7]. In addition to numerical experiments, bounds are given in [7] on the mean square error of the approximate solution $\tilde{X}$ at time $t=\tau$. We note that it is not possible to conclude that functionals of X can be estimated from samples of $\tilde{X}$ based solely on mean square error of $\tilde{X}(\tau)$. This conclusion holds if $\tilde{X}$ converges weakly to X.

The weak convergence of the sequence of processes X_n in Eq. (4) to X in Eq. (1) guarantees the convergence of distributions of functionals of X_n to those of corresponding functionals of X. A numerical illustration of this convergence is provided by the following example. Suppose X is a filtered Poisson process, that is, it is the solution of Eq. (1) with $\mu[X(t)]=-\rho X(t)$, $\rho>0$, and $\sigma[X(t)]=1$, and that our objective is to find the distribution of the random variable $\max_{\tau_1\le t<\tau_2}|X(t)|$, $0\le\tau_1<\tau_2$. Let T_k be the jump times of C in Eq. (2) and denote by $X(T_k)$ the value of X immediately following the kth jump of C. We have

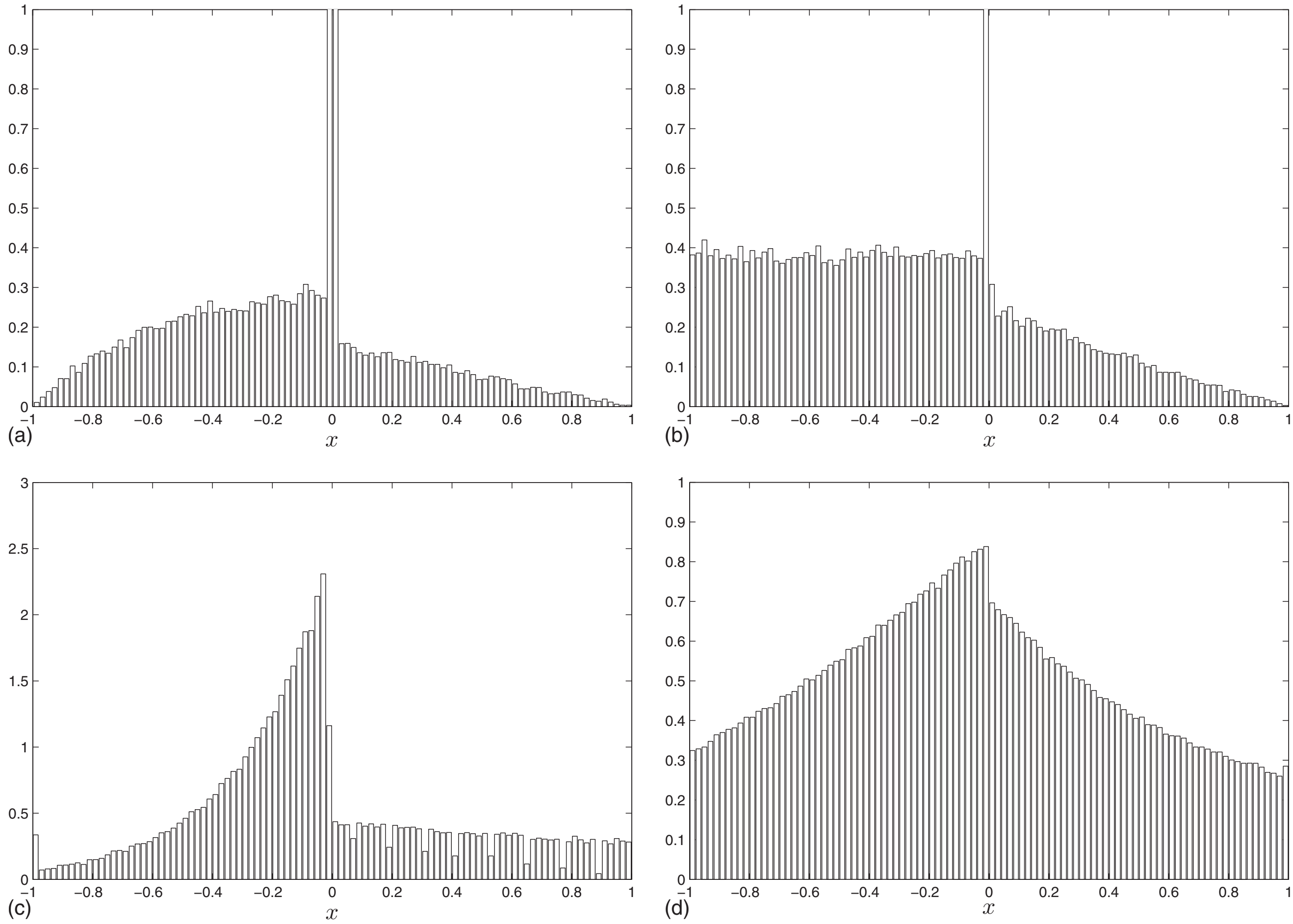

FIG. 1. Histogram of stationary state $X_{n,k}$ for (a) $\lambda=0.5$, (b) $\lambda=1$, (c) $\lambda=2$, and (d) $\lambda=100$.

$$X(T_k) = X(T_{k-1})e^{-\rho(T_k-T_{k-1})} + Y_k, \quad k = 1,2, \ldots , \qquad (28)$$

and $\max_{t\in(\tau_1,\tau_2]}|X(t)|=\max_{T_k\in(\tau_1,\tau_2]}|X(T_k)|$ almost surely (a.s) by properties of filtered Poisson processes. The recurrence formula in Eq. (28) can be used to generate samples $X(T_k)$, calculate the corresponding samples of $\max_{T_k\in(\tau_1,\tau_2]}|X(T_k)|$, and construct histograms of this random variables. Alternatively, the fixed time step recurrence formula in Eq. (4) can be used to generate samples of $X_{n,k}$, calculate the corresponding samples of $\max_{t_k\in(\tau_1,\tau_2]}|X_{n,k}|$, and construct histograms of this variable. The numerical results in Fig. 2 are for $\tau_1=10$, $\tau_2=20$, $\lambda=\rho=1$, and Gaussian jumps Y_k with mean 0 and variance $E[Y_1^2]=2\rho/\lambda$, so that X in the stationary regime has mean 0 and variance 1. The histograms of $\max_{t_k\in(\tau_1,\tau_2]}|X_{n,k}|$ and $\max_{T_k\in(\tau_1,\tau_2]}|X(T_k)|$ are shown in the left and the right panels in Fig. 2, and are based on 10 000 independent

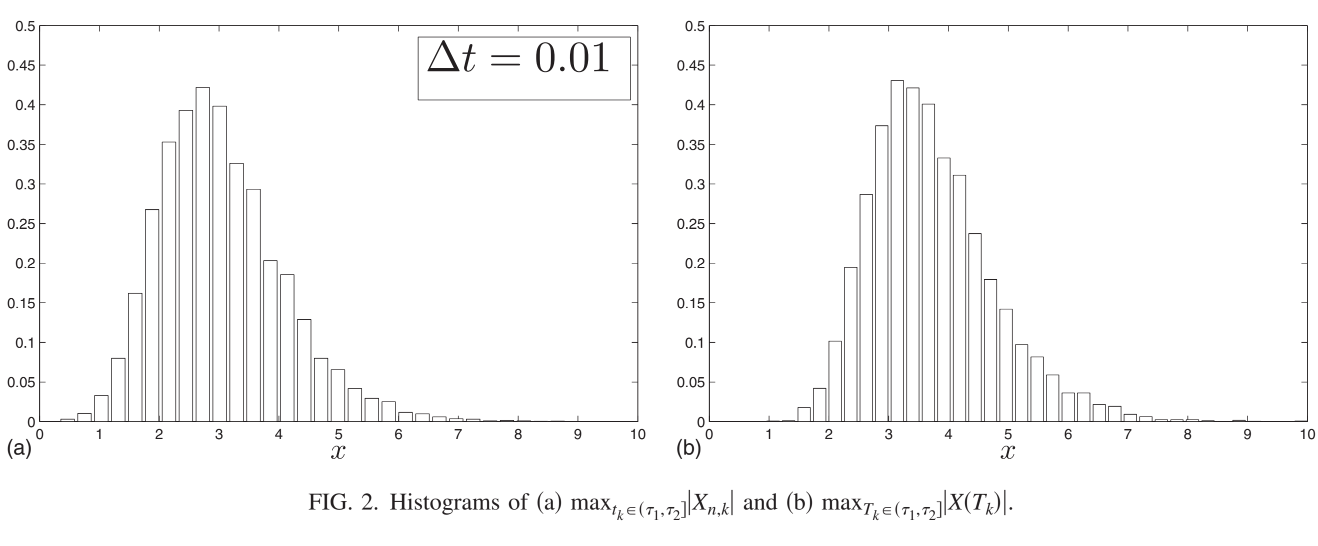

FIG. 2. Histograms of (a) $\max_{t_k\in(\tau_1,\tau_2]}|X_{n,k}|$ and (b) $\max_{T_k\in(\tau_1,\tau_2]}|X(T_k)|$.

samples of these processes. Since there is no analytical solution for the distribution of $\max_{t\in(\tau_1,\tau_2]}|X(t)| = \max_{T_k\in(\tau_1,\tau_2]}|X(T_k)|$, the histogram of $\max_{T_k\in(\tau_1,\tau_2]}|X(T_k)|$ is taken as reference for assessing the accuracy of the fixed time step recurrence formula. The similarity of the results in the two panels of Fig. 2 demonstrate the accuracy of the fixed time step method even when used to characterize functionals of the solution of stochastic differential equations driven by Poisson white noise.

B. Lévy white noise

Consider the special case of Eq. (1) with $\mu[X(t)]=-X(t)^3$ and $\sigma[X(t)]=1$ and $Y=L_\alpha$. This equation has a strong unique solution $X(t)$ that becomes stationary as time increases indefinitely [17]. The characteristic function $\varphi(u)=E\{\exp[iuX(t)]\}$ of $X(t)$ in the stationary regime satisfies the ordinary differential equation $u\varphi'''(u)-|u|^\alpha\varphi(u)=0$ accompanied by the boundary conditions $\varphi(0)=1$ and $\varphi'(0)=0$ and the requirement $|\varphi(u)|\le 1$, $u\in\mathbb{R}$. The solution of this equation for $\alpha=1$ is

$$\varphi(u)=e^{-|u|/2}[\cos(\sqrt{3}u/2)+\sin(\sqrt{3}|u|/2)/\sqrt{3}], \quad u\in\mathbb{R}, \tag{29}$$

so that the stationary marginal density of $X(t)$ has the expression

$$f(x)=\frac{1}{\pi(a_1^2+1/4)(a_2^2+1/4)}, \quad x\in\mathbb{R}, \tag{30}$$

where $a_1=x+\sqrt{3}/2$ and $a_2=-x+\sqrt{3}/2$ [17].

We generate samples of X by the recurrence formula in Eq. (4) in a time interval $[0,\tau]$ sufficiently long for the process to reach stationarity, use samples of $X_n(\tau)$ to construct a histogram of the stationary state, and compare the resulting histogram with the stationary density $f(x)$ in Eq. (30). The application of the recurrence formula in Eq. (4) requires to select a threshold $a>0$, a shape parameter α, and calculate the properties of the Gaussian and the Poisson components of the driving noise. For $\alpha=1$, the scale of the Gaussian noise is $\gamma(1,a)=\sqrt{2\pi/a}$ by Eqs. (14) and (12). The compound Poisson process $C^{(1,a)}$ in Eq. (13) is defined by the Poisson counting process $N^{(1,a)}$ with intensity $\lambda^{(1,a)}=2/(\pi a)$ and jumps $Y_k^{(1,a)}$ following the distribution

$$F_a(y)=\frac{a}{2}\left[\frac{1}{|y|}1(y<-a)+\frac{1}{a}1(y\ge -a)+\frac{1-a/y}{a}1(y\ge a)\right], \quad y\in\mathbb{R}. \tag{31}$$

The resulting integration formula is

$$X_{n,k}=X_{n,k-1}-X_{n,k-1}^3\Delta t_n+\sqrt{\frac{2\pi}{a}}\Delta t_n^{1/2}G_{k-1}+V_{n,k-1}^{(1,a)}, \quad k=1,2,\ldots, \tag{32}$$

where $\{G_{k-1}\}$ are independent standard Gaussian variables and $\{V_{n,k-1}^{(1,a)}\}$ are independent identically distributed random variables that have the distribution F_a in Eq. (31) with probability $p_{n,\alpha,a}=1-\exp(-\lambda^{(\alpha,a)}\Delta t_n)$ and are equal to 0 with probability $1-p_{n,\alpha,a}$.

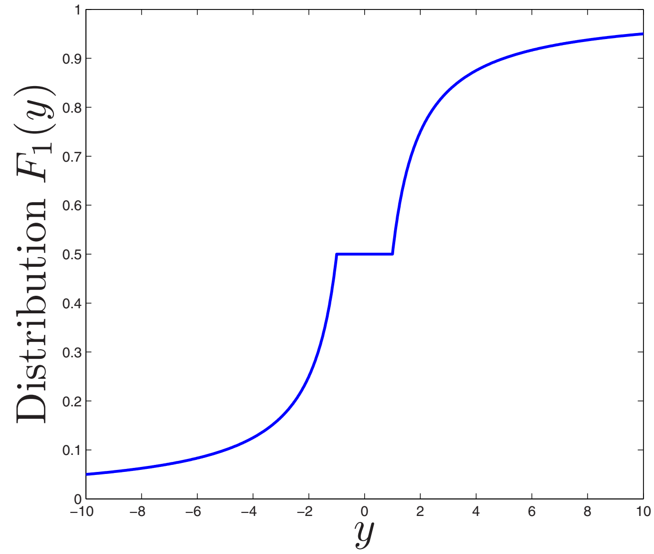

FIG. 3. (Color online) Distribution F_1 in Eq. (31) for $\alpha=1$ and $a=1$.

Numerical results in the following figures are for $\tau=5$, $\Delta t_n=0.0001$, and $\alpha=1$. Figure 3 shows the distribution function in Eq. (31) in the range $[-10,10]$, that is, the distribution of the jumps of the Poisson component of L_α. The plot suggests that F_1 has heavy tails. Figure 4 shows a sample of X generated by the recurrence formula in Eq. (32). The sample exhibits jumps that are caused by the jumps of the Poisson component $C^{(\alpha,a)}$ of the Lévy noise L_α. The jumps of X are spaced in time at $1/\lambda^{(1,a)}=\pi a/2$ on average. The sample varies continuously between jumps since only the Brownian component $\gamma(\alpha,a)B$ of L_α is active during the time between consecutive jumps of $C^{(\alpha,a)}$.

Figure 5 shows histograms of $X(\tau)$ constructed from 100 000 independent samples of $X_{n,k}$ at time $\tau=5$ that have been generated by the recurrence formula in Eq. (32) with time step $\Delta t_n=0.0001$ for two thresholds: (*a*) $a=0.5$ (left

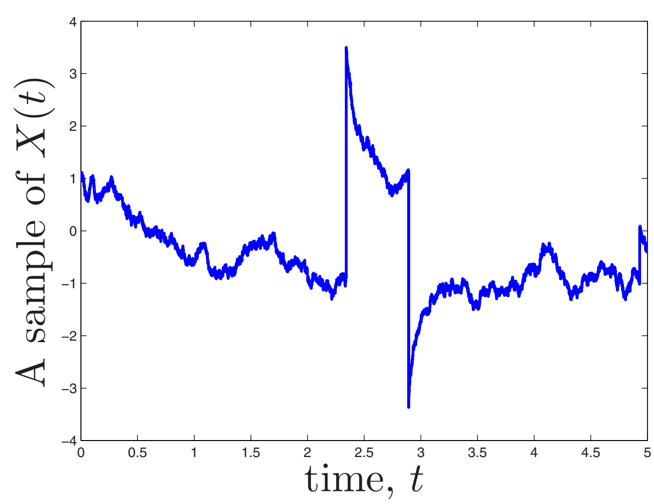

FIG. 4. (Color online) A sample of $X(t)$ generated by Eq. (32).

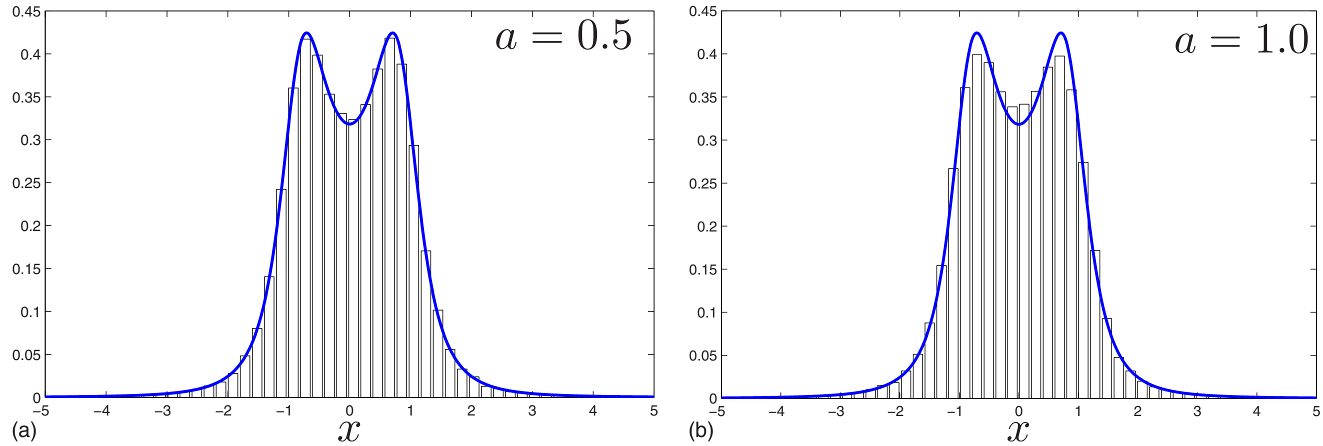

FIG. 5. (Color online) Histogram of $X_{n,k}$ for (*a*) $a=0.5$ and (*b*) $a=1.0$ and the density of $X(t)$ in Eq. (30).

panel) and (*b*) $a=1.0$ (right panel). The continuous line in the figure is the stationary density of X given by Eq. (30). The histogram of $X_{n,k}$ traces closely the density in Eq. (30) for both values of a. We also note that, as for SDE's with PWN-,statistics of functionals of X can be calculated approximately from samples of X_n since X_n converges weakly to X.

VI. CONCLUSIONS

A fixed time step method has been developed for integrating stochastic differential equations driven by Poisson white noise (PWN) and Lévy white noise (LWN). The method is similar to that proposed in [7] for integrating stochastic differential equations with PWN but has been developed using different arguments. We have interpreted PWN as the formal derivative of a compound Poisson process C while LWN has been viewed as the formal derivative of an α-stable Lévy process L_α. Fixed time step algorithms for integrating stochastic differential equations (SDE's) with PWN have been obtained from approximations of C by random walks. The construction of fixed time step integration algorithms for SDE's with LWN was based on the integration scheme developed for SDE's with PWN and a representation of L_α by a sum of a scaled Brownian motion and a compound Poisson process.

Numerical experiments were used to demonstrate the implementation and the accuracy of the proposed integration algorithms for SDE's with PWN and LWN. Moreover, it was shown that the sequence of approximating solutions of a SDE corresponding to refining approximations of PWN and LWN converges weakly to the exact solutions of these equations. This convergence implies that marginal statistics as well as distributions of functionals of the exact solution of a SDE can be estimated from samples of approximate solutions of this equation delivered by the integration algorithms in this study.

APPENDIX

The weak convergence of both C_n and X_n to C and X, respectively, needs to be studied in the space $D[0,\tau]$ of real-valued functions that are right continuous and have left limits since the samples of these processes have jumps.

Convergence $C_n \Rightarrow C$. We have seen that the finite dimensional distributions of C_n converge to those of C. To prove the weak convergence of C_n to C, we need to show that the sequence of processes $\{C_n\}$ is tight. According to a result in [21] (Theorem 15.2), $\{C_n\}$ is tight if the following two conditions are satisfied.

First, we need to show that for every $\eta>0$, there exists a threshold $a>0$ such that $P[\sup_{0\le t\le\tau}|C_n(t)|>a]\le\eta$ for all $n\ge 1$. We only show that this condition is satisfied for the special case in which the jumps $\{Y_k\}$ of C have a symmetric distribution. In this case, we have

$$\begin{aligned} P[\sup_{0\le t\le\tau}|C_n(t)|>a] &\le P[\sup_{0\le t\le\tau} C_n(t)>a] \\ &\quad + P[\inf_{0\le t\le\tau} C_n(t)<-a] \\ &= 2P[\sup_{0\le t\le\tau} C_n(t)>a] \end{aligned} \tag{A1}$$

and

$$\begin{aligned} P[C_n(\tau)>a] &= P[C_n(\tau)>a|T_n(a)\le\tau]P[T_n(a)\le\tau] \\ &\le \frac{1}{2}P[T_n(a)\le\tau] \end{aligned} \tag{A2}$$

for $T_n(a)=\inf\{t:C_n(t)>a\}$, where the latter inequality follows from the symmetry of the marginal distribution of $C_n(t)$. Since

$$P[T_n(a)\le\tau] = P[\sup_{0\le t\le\tau} C_n(t)>a] = 2P[C_n(\tau)>a], \tag{A3}$$

we have $P[\sup_{0\le t\le\tau}|C_n(t)|>a]\le 4P[C_n(\tau)>a] \le 4E[C_n(\tau)^2]/a^2$ using also the Chebyshev inequality $P[C_n(\tau)>a]\le E[C_n(\tau)^2]/a^2$. Accordingly, the required condition is satisfied, if we set $a=\{4E[C_n(\tau)^2]/\eta\}^{1/2}$ for any $\eta>0$.

Second, we need to show that for each $\varepsilon>0$ and $\eta>0$, there exists $\delta\in(0,1)$ and an integer n_0 such that $P[W_n'(\delta)\ge\varepsilon]\le\eta$ for $n\ge n_0$, where $W_n'(\delta)=\inf_{\{s_i\}}\max_{0<i\le r} W_n[t_{i-1},t_i)$, $0\le t_0<t_1<\cdots<t_r=\tau$ is a partition of $[0,\tau]$ such that $t_i-t_{i-1}>\delta$, and

$W_n(\delta)=\sup\{|C_n(s')-C_n(s'')|:s',s''\in[t,t+\delta]\}$. Since $W_n'(\delta)\le\max_{1\le k\le n}|V_{n,k}|$ for any $\delta\in(0,1)$, we have $P(W_n'(\delta)>\varepsilon)\le P(\max_{1\le k\le n}|V_{n,k}|>\varepsilon)$. Let $\bar{F}$ denote the distribution of $|Y_1|$. We have

$$P(\max_{1\le k\le n}|V_{n,k}|\le\varepsilon)=P(|V_{n,1}|\le\varepsilon)^n\ge e^{-\lambda\tau}[1+\lambda\Delta t_n\bar{F}(\varepsilon)]^n \tag{A4}$$

so that $P[W_n'(\delta)>\varepsilon]\le P(\max_{1\le k\le n}|V_{n,k}|>\varepsilon)\le 1-e^{-\lambda\tau}[1+\lambda\tau\bar{F}(\varepsilon)/n]^n$. Since this upper bound on $P[W_n'(\delta)>\varepsilon]$ is a decreasing function of n, we can find an n_0 such that $P[W_n'(\delta)>\varepsilon]\le\eta$ for $n\ge n_0$. In summary, both conditions of the theorem are satisfied, so that C_n converges weakly to C.

Convergence $X_n\Rightarrow X$. We use a result in [22] (Theorem 5.4) to prove this convergence, which considers the sequence of process

$$C_n^\delta(t)=C_n(t)-\sum_{0<s\le t}h_\delta[|\Delta C_n(s)|]\Delta C_n(s)=\sum_{0<s\le t}\{1-h_\delta[|\Delta C_n(s)|]\}\Delta C_n(s), \tag{A5}$$

where $h_\delta(r)=(1-\delta/r)1(r\ge\delta)$ for $\delta,r>0$. Note that $[1-h_\delta(r)]r\le 2\delta$ so that C_n^δ is bounded over any bounded time interval irrespective of the properties of the jumps of C.

Theorem 5.4 in [22] holds under two conditions. The first condition is that Y_n converges weakly to Y. This condition is satisfied since the first coordinate of Y_n and Y is the identity function and the convergence $C_n\Rightarrow C$ holds. The second condition requires that, for each $\beta>0$, there exists a sequence of stopping times $\{T_n\}$ such that $P(T_n\le\beta)\le 1/\beta$ and $\sup_n E\{[C_n^\delta(t\wedge T_n)]\}<\infty$, where $[C_n^\delta(t\wedge T_n)]$ denotes the quadratic variation of $C_n^\delta(t\wedge T_n)$. The sequence of stopping times $T_n=\inf\{t\ge 0:\sum_{k=1}^{[t/\Delta t_n]}V_{n,k}^2>a\}$ for $a>0$ has the required property since

$$P(T_n\le t)=P\left(\sum_{k=1}^{[t/\Delta t_n]}V_{n,k}^2>a\right)\le\frac{E\left[\sum_{k=1}^{[t/\Delta t_n]}V_{n,k}^2\right]}{a}\le\frac{\lambda t E[Y_1^2]}{a}, \tag{A6}$$

or $P(T_n\le\beta)\le 1/\beta$ for $t=\beta$ and $a=\lambda\beta^2E[Y_1^2]$. We also have $E\{[C_n^\delta(t\wedge T_n)]\}\le E\{[C_n^\delta(t)]\}\le E[\sum_{k=1}^{(t/\Delta t_n)}V_{n,k}^2]<\infty$.

Since the two conditions of Theorem 5.4 in [22] are satisfied, we conclude that the limit of X_n as $n\to\infty$, that is, the process $\lim_{n\to\infty}X_n$ satisfies the first equality in Eq. (24). Since the solution of this equation exists and is unique in our case, we conclude that X_n converges weakly to X. Accordingly, statistics of functionals of X can be approximated by those those of functionals of X_n.

[1] W. Horsthemke and R. Lefever, Phys. Lett. A **64**, 19 (1977).
[2] M. Grigoriu, *Stochastic Calculus. Applications in Science and Engineering* (Birkhäuser, Boston, 2002).
[3] R. S. Bucy and P. D. Joseph, *Filtering for Stochastic Processes with Applications to Guidance* (Chelsea Publishing Company, New York, 1987).
[4] P. A. Ruymgaart and T. T. Soong, *Mathematics of Kalman-Bucy Filtering* (Springer-Verlag, New York, 1988).
[5] P. D. Ditlevsen, Phys. Rev. E **60**, 172 (1999).
[6] S. Chaumout, P. Imkeller, M. Müller, and U. Horst, private communication.
[7] C. Kim, E. K. Lee, P. Hänggi, and P. Talkner, Phys. Rev. E **76**, 011109 (2007).
[8] M. Grigoriu, J. Sound Vibrat. **198**, 193 (1996).
[9] R. Iwankiewicz and S. Nielsen, Dynamic response of nonlinear systems to Poisson-distributed random impulses.
[10] M. Grigoriu, Phys. Lett. A **217**, 258 (1996).
[11] P. E. Kloeden and E. Platen, *Numerical Solutions of Stochastic Differential Equations* (Springer–Verlag, New York, 1992).
[12] D. J. Higham and P. E. Kloeden, Numerische Mathematik **101**, 101 (2005).
[13] P. Protter and D. Talay, Ann. Probab. **25**, 393 (1997).
[14] J. Jacod, Ann. Probab. **32**, 1830 (2004).
[15] S. Asmussen and J. Rosiński, J. Appl. Probab. **38**, 482 (2001).
[16] G. Samorodnitsky and M. S. Taqqu, *Stable Non-Gaussian Random Processes* (Stochastic Models with Infinite Variance, Birkhäuser, New York, 1994).
[17] G. Samorodnitsky and M. Grigoriu, Theor. Math. Phys. **150**, 332 (2007).
[18] B. Dybiec, E. Gudowska-Nowak, and P. Hänggi, Phys. Rev. E **75**, 021109 (2007).
[19] B. Dybiec, E. Gudowska-Nowak, and P. Hänggi, Phys. Rev. E **73**, 046104 (2006).
[20] M. Grigoriu, *Applied Non-Gaussian Processes: Examples, Theory, Simulation, Linear Random Vibration, and MATLAB Solutions* (Prentice Hall, Englewoods Cliffs, NJ, 1995).
[21] P. Billingsley, *Convergence of Probability Measures* (John Wiley and Sons, Inc., New York, 1968).
[22] T. G. Kurtz and P. Protter, Ann. Probab. **19**, 1035 (1991).